Geoderma 401 (2021) 115342

Contents lists available at ScienceDirect

Geoderma

journal homepage: www.elsevier.com/locate/geoderma

Crop straw incorporation mediates the impacts of soil aggregate size on greenhouse gas emissions

Mengdie Jiang [a], Niping Yang [a,b], Jinsong Zhao [a,c,*], Muhammad Shaaban [d,e], Ronggui Hu [a,c,*]

[a] College of Resources and Environment, Huazhong Agricultural University, Wuhan 430070, China
[b] Shenzhen PowerSmart Technology Co. Ltd., Shenzhen 518057, China
[c] State Environmental Protection Key Laboratory of Soil Health and Green Remediation, Wuhan 430070, China
[d] Institute of Mountain Hazards and Environment, Chinese Academy of Sciences, Chengdu 610041, China
[e] Department of Soil Science, Faculty of Agricultural Sciences and Technology, Bahauddin Zakariya University, Multan, Pakistan

ARTICLE INFO

Handling Editor: Daniel Said-Pullicino

Keywords:
CO_2 emission
N_2O emission
Soil aggregate
Straw addition
Enzyme activities

ABSTRACT

Greenhouse gas (GHG) emissions from agricultural soil have been widely discussed to combat the risks of global warming. However, GHG emissions at the soil aggregate scale have yet to be elucidated, particularly in association with straw incorporation. In this study, three different sizes of soil aggregates (1–2, 0.25–1, and < 0.25 mm) were incubated in the laboratory at 25 °C for 58 days with and without rapeseed straw (*Brassica napus* L.) addition to determine the extent to which aggregate sizes contribute mostly to carbon dioxide (CO_2) and nitrous oxide (N_2O) emissions upon straw addition. Results showed that cumulative CO_2 emission in < 0.25 mm fraction (546 mg C kg^{-1} soil) was significantly ($P < 0.001$) lower than that in 0.25–1 mm (810 mg C kg^{-1} soil) and < 1–2 mm (762 mg C kg^{-1} soil) fractions in straw-unamended treatments. Straw addition increased cumulative CO_2 emissions by 7.2-, 5.87-, and 13.1-fold from 1 to 2, 0.25–1, and < 0.25 mm fractions, respectively, compared with those of the corresponding straw-unamended treatments. Straw addition increased cumulative N_2O emissions in each size of aggregates, and cumulative N_2O emissions in 1–2 mm fraction ranked the first across the straw-unamended and straw-amended treatments. The activities of β-glucosidase, β-cellobiohydrolase, N-acetyl-β-D-glucosaminidase, and leucine aminopeptidase were enhanced by straw addition in each size of aggregates, and < 0.25 mm fraction exerted the lowest enzyme activities. Structural equation modeling and redundancy analysis confirmed that the interaction between soil physiochemical parameters (nitrate nitrogen and dissolved organic C) and specific enzyme activities was the key driver for regulating CO_2 and N_2O emissions. These results implied that identifying the straw as a function of aggregate-scale GHG dynamics could improve the mechanistic understanding of global warming.

1. Introduction

The increasing amount of atmospheric greenhouse gases (GHGs), i.e., carbon dioxide (CO_2) and nitrous oxide (N_2O), pose great challenge to climate change and global warming (Chabbi et al., 2017). Although the concentration of N_2O is lower than that of CO_2, the much greater radiative forcing of N_2O (298-fold) over a 100-year time horizon has aggravated global warming (IPCC, 2014). The exchange of GHGs at the soil–atmosphere interface is driven by microbial activities and inevitably moderated by soil physicochemical properties (Han and Zhu, 2020). GHG emissions are dominantly controlled by soil physicochemical factors, i.e., soil temperature, moisture, pH, pore size distribution, structure, and carbon (C) and nitrogen (N) contents in soil (Bandyopadhyay and Lal, 2014; Garcia-Marco et al., 2014; Kimura et al., 2012; Zhou et al., 2017).

Soil aggregates are grouped in terms of different sizes and implicated in mediating soil physicochemical processes (Zhao et al., 2017). Microbial extracellular polysaccharides induce microaggregates to form free primary particles, reaching approximately 1 μm in diameter, and hold each microaggregate together reiteratively up to about 0.25 mm (Bronick and Lal, 2005b). On a grander scale, organo-mineral complexes physically bind agents (e.g., fine roots and fungal hyphae) to macroaggregates with a size of > 0.25 mm (Bronick and Lal, 2005b). The distinct characteristics of the mean pore size, substrate chemical composition, and microbial community composition in each sized aggregate result in small-scale heterogeneity in gaseous production and movement in soil

* Corresponding authors.
E-mail addresses: jszhao@mail.hzau.edu.cn (J. Zhao), rghu@mail.hzau.edu.cn (R. Hu).

https://doi.org/10.1016/j.geoderma.2021.115342
Received 21 December 2020; Received in revised form 23 June 2021; Accepted 5 July 2021
Available online 12 July 2021

(Upton et al., 2019; Wang et al., 2019a). As reported by recent studies, changes in soil aggregate sizes can affect the activities of nitrifiers and denitrifiers (Li et al., 2019, 2020; Zhang et al., 2021), causing differences in soil N_2O emissions. However, studies have presented conflicting results on CO_2 and N_2O releases among differently sized aggregates. Most studies have shown that macroaggregates (>0.25 mm) yield higher levels of CO_2 and N_2O than microaggregates (<0.25 mm; Bandyopadhyay and Lal, 2014; Jayarathne et al., 2021; Ley et al., 2018; Robinson et al., 2014; Wang et al., 2019a). Other studies have indicated opposite views in some cases (Mangalassery et al., 2013; Reeves et al., 2019; Uchida et al., 2008). Furthermore, explicit trends have yet to be drawn.

Studies on the effects of soil aggregate size have separately focused on CO_2 and N_2O emissions. Therefore, further studies should be performed to reveal aggregate-scale GHG dynamics, which is critical for the understanding of the mechanisms regulating GHG emissions and mitigating climate change.

The huge crop straw produced in China is almost one-third of the world's production and can directly pose an air quality problem if it is burned in an open field (Li et al., 2017). In this context, partial or full straw returning has been recommended to maintain soil productivity and alleviate the negative influence of combustion on climate. The returning of straw can also be relevant for the increasing importance of various initiatives, such as those aiming to increase soil organic C (SOC) stocks (Liu et al., 2014; Soussana et al., 2019) or circular economy (Cantzler et al., 2020). The importance of aggregates on soil functions increases when crop straw is incorporated in soil because crop straw returning can alter soil aggregate-size distribution and associated C storage (Wang et al., 2019c). Fresh straw incorporation promotes the generation of soil binding agents, such as protein, polysaccharides, and microbe-derived gelatinous substances; consequently, it helps soil microaggregates bind to macroaggregates (Huang et al., 2018). Furthermore, Messiga et al. (2011) showed that straw returning also increases the aggregate-associated C content of all sizes, especially in macroaggregates. Therefore, the effect of aggregate sizes on GHG emissions may be related to the influence of crop straw returning. Previous studies only focused on GHG fluxes from bulk soils in response to crop straw addition (Wang et al., 2019b). For example, crop residue input in soil can provide sufficient amount of easily decomposable and energy-rich substrates for soil microbes, resulting in either the acceleration or suppression of existing SOC decomposition (Wu et al., 2019). Crop residues are preferentially allocated to microbial biomass (anabolism), whereas the remaining crop residues are lost to the atmosphere as CO_2 through respiration (catabolism; Mehnaz et al., 2019). The two primarily microorganism-mediated processes of N_2O production in soils are nitrification and denitrification (Wrage et al., 2001). Once incorporated, crop residues often stimulate the growth of soil nitrifying and denitrifying microbes, thereby strongly influencing N_2O emissions (Zhou et al., 2020).

Studies have focused on the response of CO_2 and N_2O emissions to crop straw incorporation or different aggregate sizes in an isolated manner. Therefore, further studies should investigate the underlying mechanisms driving aggregate sizes in relation to CO_2 and N_2O emissions upon crop straw addition. Here, we hypothesized that 1) straw addition would increase labile C, N, and enzyme activities, consequently increasing CO_2 and N_2O emissions in each soil aggregate size, and 2) an interaction would occur between soil aggregate size and straw. As such, the increase in CO_2 and N_2O emissions with straw addition would be greater in large aggregates, which were associated with high labile C, N, and enzyme activities. To test these hypotheses, we performed a laboratory experiment by using three different sizes of soil aggregates (1–2, 0.25–1, and < 0.25 mm) combined with rapeseed straw. Extracellular enzyme activities are great indices of microbially driven organic compound decomposition because of their rapid response to environmental changes (Nie et al., 2014; Sinsabaugh et al., 2002). Changes in the activities of soil extracellular enzymes (β-glucosidase [BG], β-cellobiohydrolase [CB], N-acetyl-β-D-glucosaminidase [NAG], and leucine aminopeptidase [LAP], phenoloxidase [po] and peroxidase [per]), involved in soil C and N mineralization were further monitored to explore the underlying mechanisms of the observed varying GHG emissions induced by soil aggregate sizes upon straw addition. Our integrated laboratory experiment aimed to (1) investigate the responses of CO_2 and N_2O emissions and soil enzyme activities to differently sized soil aggregates upon straw addition and (2) elucidate the underlying mechanisms of how soil aggregate sizes interacted with straw addition driving GHG emissions. This study provided a basis for lessening the large uncertainties in GHG exchanges because of soil heterogeneity and for evaluating the combined climatic impact of GHGs at the soil aggregate scale.

Table 1
Properties of bulk soil and differently sized soil aggregates.

Soil properties	Bulk soil	Aggregate fractions		
		1–2 mm	0.25–1 mm	< 0.25 mm
TC (g kg^{-1})	16.52 ± 0.06	17.31 ± 0.00	17.00 ± 0.04	15.20 ± 0.02
TN (g kg^{-1})	1.91 ± 0.01	2.21 ± 0.03	2.10 ± 0.00	1.73 ± 0.02
DOC (mg kg^{-1})	38.19 ± 3.42	48.17 ± 2.20	40.35 ± 0.98	42.82 ± 2.96
NH_4^+-N (mg kg^{-1})	3.56 ± 0.06	4.69 ± 0.67	3.02 ± 0.77	3.81 ± 0.07
NO_3^--N (mg kg^{-1})	14.10 ± 0.10	20.80 ± 1.00	16.20 ± 1.70	19.10 ± 0.90
Aggregate proportion (%)	–	12	13	28

Abbreviations: TC, total carbon; TN, total nitrogen; DOC, dissolved organic carbon; NH_4^+-N, ammonia nitrogen; NO_3^--N, nitrate nitrogen. Values are means ± standard errors ($n = 3$).

2. Materials and methods

2.1. Soil and crop straw processing

The soil used in the study was obtained from the surface layer (0–15 cm) of an upland

field (112°10′ N, 30°13′ E) in Buhe Town, Hubei Province, China. The climate is characterized as typical subtropical monsoon climate, and the annual mean air temperature and precipitation are 17.9 °C and 1055 mm, respectively. The studied soil was developed from an alluvium parent material and classified as fluvo-aquic according to the Genetic Soil Classification of China (Xi et al., 1998) or Fluvisol according to the World Reference Base for soil resources (IUSS Working Group WRB, 2015). The topsoil (0–15 cm) was characterized by silty loam texture (10% clay, 42% silt, and 48% sand), and the pH and bulk density of bulk soil were 7.31 (H_2O) and 1.4 g cm^{-3}, respectively.

The soil samples were air dried, and large dry lumps were carefully broken apart along the planes of weakness with a rubber hammer. After the recognizable organic debris and stones were gently removed, the soils were placed evenly on a set of sieves with 2, 1, and 0.25 mm openings. The sieve set was placed on a mechanical rotary shaker at a shaking frequency of 1 oscillation s^{-1} for 30 min, ultimately generating three differently sized aggregates: 1–2, 0.25–1, and < 0.25 mm. The properties of different fractions of soil aggregates and bulk soil are shown in Table 1. The rapeseed straw (*Brassica napus* L.) was collected from an experimental field at Huazhong Agricultural University (30°27′ N, 114°16′ E), Wuhan, China. The collected straws were oven dried at 60 °C to a constant weight, chopped, ground coarsely to<1 mm with a mill grinder, and divided into two portions. One portion was stored in a desiccator until it was used, and the other portion was used to measure total C (TC) and total N (TN) by using a C/N elemental analyzer (Vario PYRO, Elementar, Germany). The TC and TN contents of rapeseed straw were 368.3 and 20.3 g kg^{-1} dry biomass, respectively.

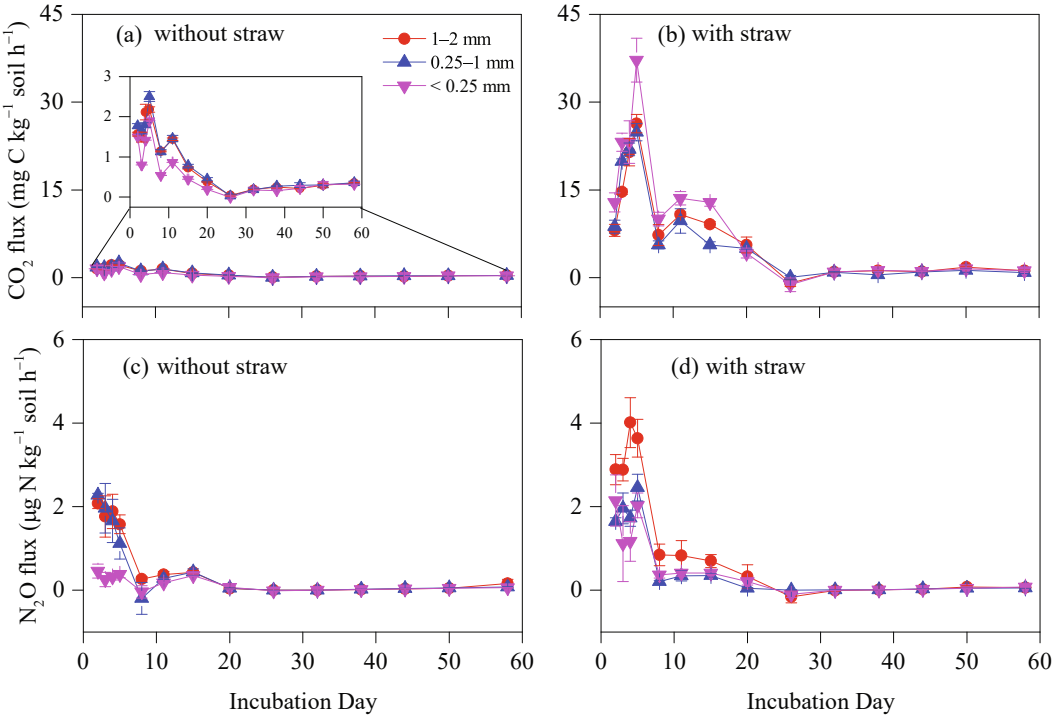

Fig. 1. The dynamics of CO_2 (a, b) and N_2O (c, d) fluxes in different soil aggregate sizes with and without straw addition over a 58-day incubation. The vertical bars in the panel represent the standard error of the mean ($n = 3$). Abbreviations: CO_2, carbon dioxide; N_2O, nitrous oxide.

2.2. Experimental design

The soil aggregate samples of three fractions (1–2, 0.25–1, and < 0.25 mm) and bulk soil were pre-incubated at 25 °C for 7 days with the soil moisture of 50% water-filled pore space (WFPS) to achieve soil microbial stabilization (Butterly et al., 2010).

After pre-incubation, soil was moistened to 60% WFPS, which is an adequate moisture content to obtain the maximum N_2O fluxes (Pilegaard, 2013) by spraying with sterile deionized water. The three soil aggregate fractions and bulk soil were treated with and without straw addition. The added rapeseed straws were carefully mixed with soil at a rate of 10 mg g^{-1} dry soil. Each of the treatments was built by weighing 20 g of soil (dry weight basis) into a 50 mL polypropylene tube. A set of eight tubes of each treatment was transferred into a 1 L glass jar for gas emission analysis. Another set of 15 tubes of each treatment was also transferred into 1 L glass jars for destructive soil sampling. All the treatments were replicated three times. All the jar tops were wrapped with polyethylene film with some pinholes to allow air exchange and then incubated at 25 °C for 58 days in an incubator. Soil moisture was maintained at 60% of WFPS by periodically supplying water to the incubation vessels.

2.3. Gas sampling and analysis

GHG sampling was carried out on days 1, 2, 3, 4, 5, 8, 11, 15, 20, 26, 32, 38, 44, 50, and 58 of the incubation. The gases were sampled in accordance with the approach of Shaaban et al. (2019). The headspace of each jar was first purged with fresh air for about 15 min after the polyethylene film was removed. The jars were hermetically sealed by using the lids with a rubber septum for gas collection. About 30 mL of gas was obtained from the headspace by using a gas-tight syringe at 0 and 1 h after jar closure. The CO_2 and N_2O concentrations were quantified through gas chromatography (GC-7890A, Agilent Technologies, USA). N_2O was detected with an electron capture detector (ECD), and CO_2 was detected with a flame ionization detector (FID; Wang and Wang, 2003). Gas fluxes were calculated from the changes in gas concentrations between 0 and 1 h after adjustments were made in accordance with the ideal gas law (Mackenzie et al., 1998). Total cumulative fluxes were estimated according to previously described methods (Kool et al., 2006).

2.4. Soil sampling and analysis

Soil was taken through destructive sampling at 1, 2, 3, 4, 5, 8, 11, 15, 20, 26, 32, 38, 44, 50, and 58 days for dissolved organic C (DOC), mineral N (NH_4^+-N and NO_3^--N), and enzyme activities analyses. Deionized water was used to extract soil DOC at a ratio of 1:5 soil:water (w:v; Shaaban et al., 2019). The mixture was shaken for 1 h before centrifugation and then filtered using a 0.45 μm filter. The extracted solution was assayed with a TOC analyzer (Vario Select, Elementar, Germany). NH_4^+-N and NO_3^--N were extracted with 1 mol L^{-1} KCl (1:5, w:v) for 1 h and filtered through ash-free filters (Shaaban et al., 2019). The extracted solution was quantified with a flow-injection analyzer (Seal Auto Analyzer, Germany). Soil pH was measured with a pH meter (Sartorius, PB-10, Germany) at a ratio of 1:2.5 soil:water (w:v). The soil TC and TN were measured using a C/N elemental analyzer (Vario PYRO, Elementar, Germany). Soil particle size (clay, silt, and sand) was analyzed using pipette methods (Kettler et al., 2001). The 100 cm^3 volumetric cutting rings were used to measure bulk density (Blake and Hartge, 1986).

The potential activities of four hydrolytic enzymes (BG, CB, NAG, and LAP) were determined in accordance with a fluorometric approach (Marx et al., 2001). 4-Methylumbelliferyl-β-D-glucopyranoside, 4-Methylumbelliferyl-β-D-cellobioside, L-Leucine-7-amino-4-methyl, and 4-Methylumbelliferyl-N-acetyl-β-D-glucosaminide were used as substrates in the assay on the activities of BG, CB, LAP, and NAG, respectively. The potential activities of two oxidative enzymes (po and per) were determined in accordance with the previous methods of Saiya-Cork et al. (2002). L-3,4-Dihydroxyphenylalanine (DOPA) substrate was used to detect po and per activities. The detailed processes of the assays for BG, CB, LAP, NAG, po, and per activities are presented in Supplementary Information.

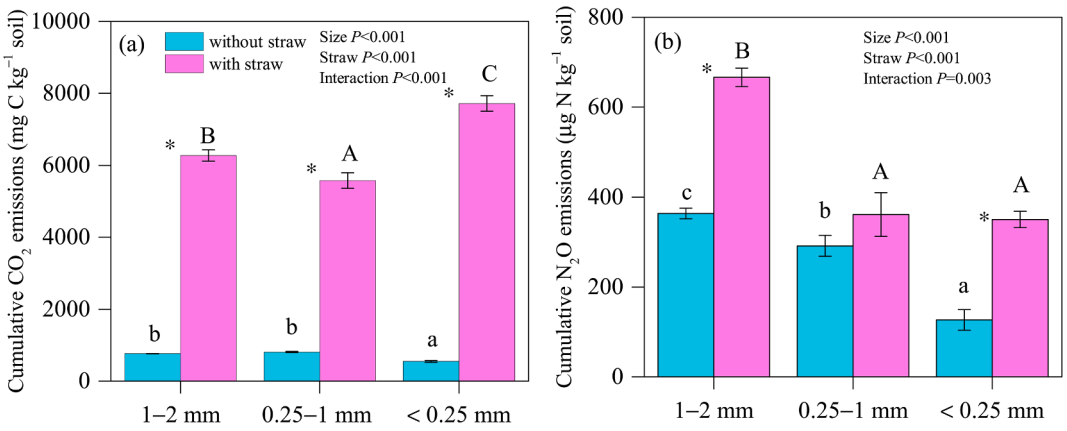

Fig. 2. Cumulative CO_2 (a) and N_2O (b) emissions in different soil aggregate sizes with and without straw addition over a 58-day incubation. Different uppercase or lowercase letters above the boxes indicate the statistical significances among aggregate sizes in treatments with or without straw addition at $P < 0.05$, respectively. * indicates the statistical significances between treatments with and without straw addition for a specific aggregate size at $P < 0.05$. The vertical bars in the panel represent the standard errors of the mean ($n = 3$). Abbreviations: CO_2, carbon dioxide; N_2O, nitrous oxide.

2.5. Contribution of soil aggregates to GHG emissions from bulk soil

The GHG emissions from individual differently sized aggregates (FB_{GHG}) were quantified with regard to GHG emissions from bulk soil in accordance with the following equation (Bandyopadhyay and Lal, 2014):

$$FB_{GHG} = F_{GHG} \times R$$

where FB_{GHG} is the GHG emission from individual aggregates (mg kg^{-1} soil), F_{GHG} is cumulative GHG emissions in individual aggregate treatments (mg kg^{-1} aggregate fraction), and R is the corresponding aggregate proportions in bulk soil (%).

The contribution (Cr) of GHG emissions from individual aggregates to GHG emissions from bulk soil was calculated with the following equation (Bandyopadhyay and Lal, 2014):

$$C_r = FB_{GHG}/B_{GHG}$$

where B_{GHG} is GHG emission from bulk soil (mg kg^{-1} bulk soil) (data not shown).

2.6. Statistical analyses

Repeated measures ANOVA was carried out to test the effects of soil aggregate size, straw addition, and interaction on soil mineral N content, DOC content, and enzyme activities. Two-way ANOVA with Duncan's test was performed to compare the differences in cumulative CO_2 and N_2O emissions between treatments. Redundancy analysis (RDA) was conducted to determine the relationships between response (CO_2 and N_2O) and explanatory variables. The explanatory variables responsible for GHG emissions were selected through best subset searching, and any model with a high multicollinearity (i.e., any variable with a variance inflation factor>10) was excluded. The coefficient of determination of the RDA model (Borcard et al., 1992) was used to divide the variation in response variables based on soil physiochemical parameters (NO_3^--N and DOC) and extracellular enzymes (BG, NAG, LAP, and po). Partial least squares structural equation modeling (PLS-SEM) was performed to further decouple the effects of soil physiochemical parameters and enzyme activities on GHG emissions because of the strong interaction effect between soil physiochemical parameters and enzyme activities on GHG emissions. Three separate PLS-SEM models for 1–2, 0.25–1, and < 0.25 mm aggregate fractions were employed to indicate the changes in the driving forces of GHG emissions. All the statistical analyses were developed in R version 4.0.2 (R Core Team, 2020), and PLS-SEM and RDA, and variation partition were performed with *vegan* (Oksanen et al., 2019) and *plspm* (Sanchez et al., 2017) package.

3. Results

3.1. CO_2 and N_2O emissions

In the straw-unamended treatments, CO_2 fluxes gradually decreased during the 58-day incubation period (Fig. 1a). The mean values of CO_2 fluxes were 0.89, 0.93, and 0.32 mg C kg^{-1} soil h^{-1} for 1–2, 0.25–1, and < 0.25 mm fractions, respectively. The CO_2 fluxes increased rapidly after straw incorporation and peaked on day 9 (Fig. 1b). The mean CO_2 fluxes from the straw-amended treatments were 7.76, 7.55, and 10.12 mg C kg^{-1} soil h^{-1} in 1–2, 0.25–1, and < 0.25 mm fractions, respectively. The soil aggregate size markedly affected cumulative CO_2 emissions ($P < 0.001$). The largest emission in 0.25–1 mm fraction and the smallest in < 0.25 mm fraction were found in the straw-unamended treatments (Fig. 2a). The interaction effect on cumulative CO_2 emissions between straw addition and soil aggregate sizes was strong ($P < 0.001$). Straw addition significantly increased cumulative CO_2 emissions in each aggregate fraction ($P < 0.001$), with a greater effect in < 0.25 mm fraction, and the cumulative CO_2 emissions in < 0.25 mm fraction was 23.3% and 38.5% higher than those in 1–2 and 0.25–1 mm fractions.

In the straw-unamended treatments, N_2O fluxes decreased from soil over time (Fig. 1c). The level of N_2O fluxes remained lower in < 0.25 mm fraction than in the other aggregate fractions during the first 11 days. The fluxes of N_2O peaked at approximately 5 days in the treatments with straw addition and then declined until the end of the incubation (Fig. 1d). The mean N_2O fluxes were 1.15, 0.64, and 0.57 μg N kg^{-1} soil h^{-1} in 1–2, 0.25–1, and < 0.25 mm fractions, respectively, which were greater than those in the straw-unamended treatments. Aggregate size ($P < 0.001$), straw ($P < 0.001$), and their interaction ($P = 0.003$) significantly affected cumulative N_2O emissions (Fig. 2b). Straw addition increased the cumulative N_2O emissions in each size of aggregates, but the significant difference was not observed in 0.25–1 mm fraction. The cumulative N_2O emission in 1–2 mm fraction was significantly higher than that in 0.25–1 and < 0.25 mm fractions across the straw-unamended and straw-amended treatments ($P < 0.001$).

In the straw-unamended treatments, cumulative CO_2 emissions in < 0.25 mm fraction had the highest contributions towards the emissions in bulk soil, followed by 0.25–1 and 1–2 mm fractions (Table S1). By contrast, cumulative N_2O emissions in the 1–2 mm fraction had the greatest contribution towards the emissions in bulk soil. The straw addition resulted in a reduction in the contribution of 1–2 and 0.25–1 mm fractions to the CO_2 and N_2O emissions of bulk soil and increased

Table 2
Probability (*P*) of soil aggregate size classes (size), straw addition (straw), incubation time (time) and their interactions on soil properties and enzyme activities based on repeated measures analysis of variance.

	DOC	NH_4^+-N	NO_3^--N	BG	CB	LAP	NAG	po	per
straw	< 0.001	< 0.001	< 0.001	< 0.001	< 0.001	< 0.001	< 0.001	0.023	ns
size	ns	ns	< 0.001	0.006	0.013	0.014	0.012	< 0.001	0.005
time	ns	< 0.001	< 0.001	< 0.001	< 0.001	< 0.001	< 0.001	< 0.001	0.006
straw × size	0.009	ns	0.015	0.001	0.006	ns	0.007	ns	ns
straw × time	< 0.001	ns	0.005	< 0.001	< 0.001	< 0.001	0.007	ns	ns
size × time	ns	ns	ns	0.035	ns	ns	ns	ns	ns
straw × size × time	ns	ns	ns	0.004	0.04	ns	ns	ns	ns

Abbreviations: DOC, dissolved organic carbon; NH_4^+-N, ammonia nitrogen; NO_3^--N, nitrate nitrogen; BG, β-glucosidase; CB, β-cellobiohydrolase; LAP, leucine aminopeptidase; NAG, N-acetyl-β-D-glucosaminidase; po, phenoloxidase; per, peroxidase. $P < 0.05$, significant; ns, not significant with $P > 0.05$.

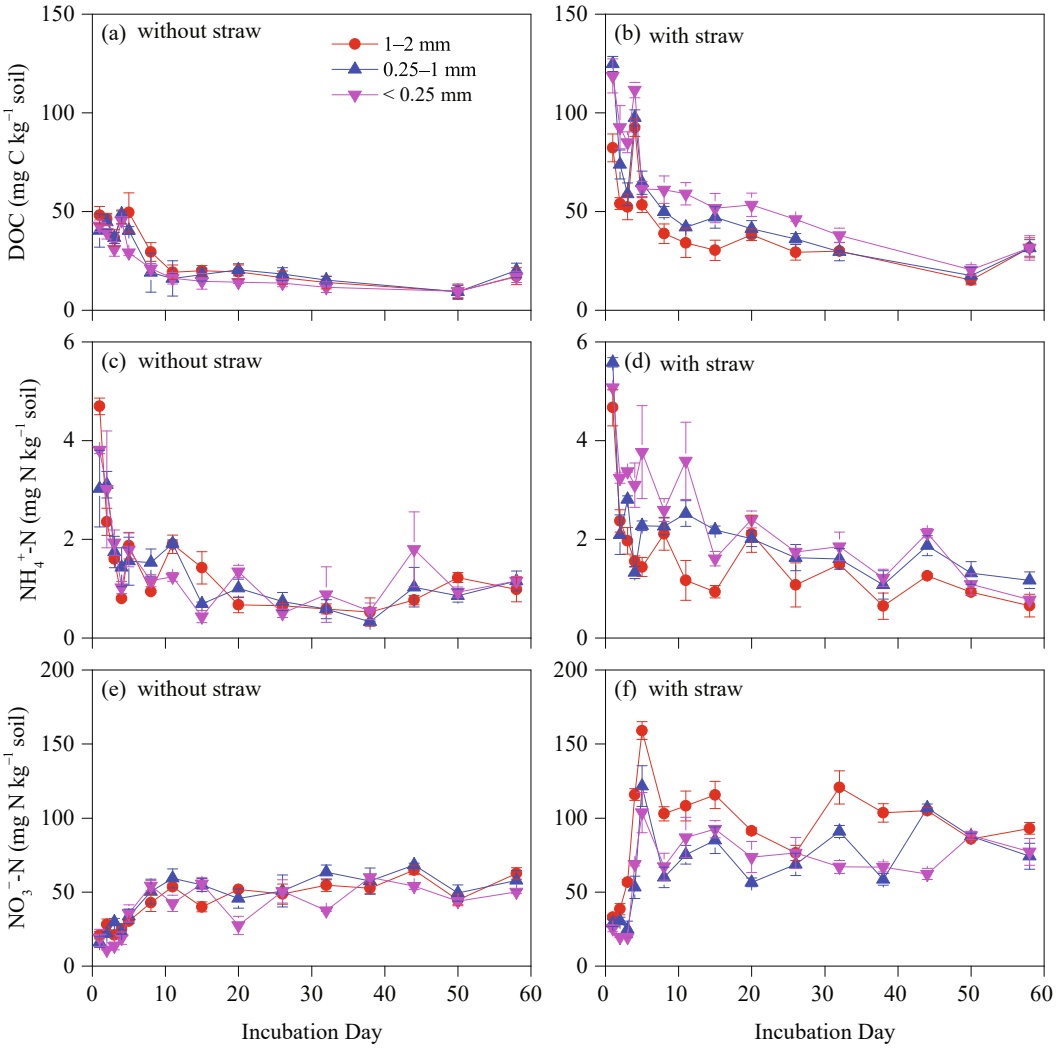

Fig. 3. The variation of soil DOC (a, b), NH_4^+-N (c, d) and NO_3^--N (e, f) contents in different soil aggregate sizes with and without straw addition over a 58-day incubation. The vertical bars in the panel represent the standard errors of the mean ($n = 3$). Abbreviations: DOC, dissolved organic carbon; NH_4^+-N, ammonia nitrogen; NO_3^--N, nitrate nitrogen.

the contribution of < 0.25 mm fraction.

3.2. Soil DOC, NH_4^+-N, and NO_3^--N content

The soil DOC content was significantly influenced by straw addition ($P < 0.001$) but not by soil aggregate size (Table 2). Their interaction obviously affected soil DOC contents ($P = 0.009$). The soil DOC contents gradually decreased during incubation (Fig. 3a and b). In the straw-unamended treatments, the highest average DOC content was observed in 1–2 mm fraction compared with that in the other fractions (Fig. 4a). Straw addition increased the average DOC contents in each aggregate, and the effect was the strongest in < 0.25 mm fraction, followed by that in the 0.25–1 mm fraction.

The soil NH_4^+-N content was only significantly influenced by straw addition ($P < 0.001$, Table 2). The NH_4^+-N contents decreased with the extension of the incubation time (Fig. 3c and d). In the samples incubated without the straw, the average NH_4^+-N were similar among three aggregate sizes (Fig. 4b). Straw addition increased the average NH_4^+-N

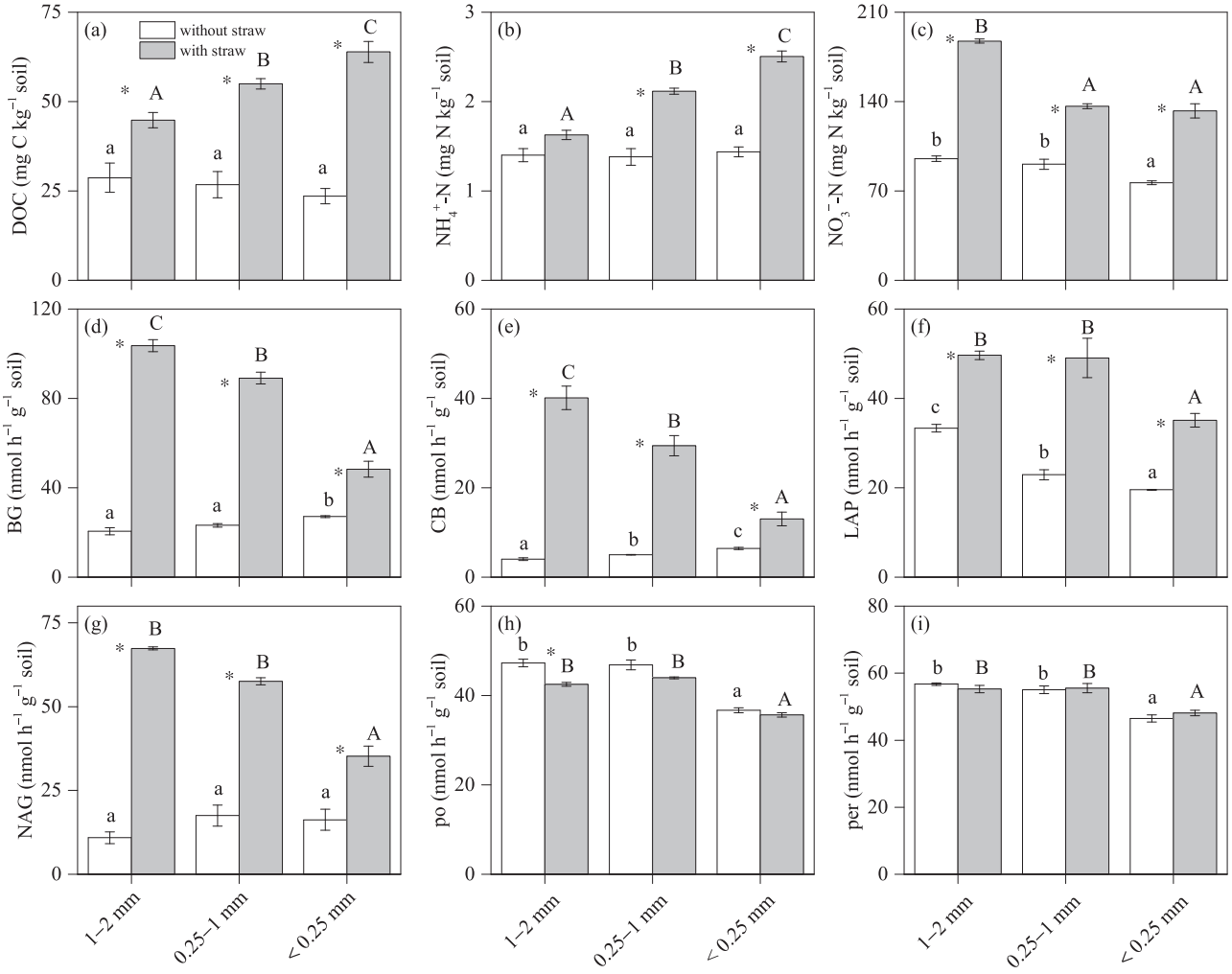

Fig. 4. Means of soil DOC, NH_4^+-N, NO_3^--N contents and enzyme activities in different soil aggregate sizes with and without straw addition over a 58-day incubation. Different uppercase or lowercase letters above the boxes indicate the statistical significances among aggregate sizes in treatments with or without straw addition at $P < 0.05$, respectively. * indicates the statistical significances between treatments with and without straw addition for a specific aggregate size at $P < 0.05$. The vertical bars in the panel represent the standard errors of the mean ($n = 3$). Abbreviations: DOC, dissolved organic carbon; NH_4^+-N, ammonia nitrogen; NO_3^--N, nitrate nitrogen; BG, β-glucosidase; CB, β-cellobiohydrolase; LAP, leucine aminopeptidase; NAG, N-acetyl-β-D-glucosaminidase; po, phenoloxidase; per, peroxidase.

contents, and the highest content was found in < 0.25 mm fraction.

Soil aggregate size, straw addition, and their interaction significantly affected the soil NO_3^--N contents (Table 2). The soil NO_3^--N contents rapidly declined during the initial 10 days, but the stable contents of NO_3^--N were found thereafter and until the end of the incubation period (Fig. 3e and f). The straw addition increased the average NO_3^--N contents in each aggregate size (Fig. 4c). Regardless of straw addition, the average NO_3^--N contents were higher in the 1–2 mm fraction than in the other fractions.

3.3. Soil extracellular enzyme activities

The activities of all the tested enzyme were significantly affected by soil aggregate size, straw addition, and their interaction ($P < 0.05$) except that the activity of per was not significantly affected by straw addition (Table 2). Straw addition resulted in a rapid increase in BG and CB during the first 11 days in 1–2 and 0.25–1 mm fractions (Fig. S1b and d). The average BG and CB activities were significantly higher in 1–2 and 0.25–1 mm fractions than in < 0.25 mm fraction in the straw-amended treatments ($P < 0.05$; Fig. 4d and e). The activities of LAP and NAG exhibited their own temporal patterns (Fig. S1e–h). The activity of LAP increased with time during the first 11 days and then decreased gradually regardless of straw addition. The NAG activity fluctuated rapidly with time. The average LAP activity in < 0.25 mm fraction was lower than that in the other fractions in the straw-unamended and straw-amended treatments (Fig. 4f). The average NAG activity in three different aggregate sizes did not significantly differ in the straw-unamended treatments (Fig. 4g). The activities of LAP and NAG were stimulated by straw amendment, where 1–2 mm fraction had the highest average LAP and NAG and < 0.25 mm fraction had the lowest (Fig. 4f and g). The lowest average po and per activities occurred in < 0.25 mm fraction in the straw-unamended and straw-amended treatments (Fig. 4h and i). No significant differences in po and per activities were found between 1 and 2 and 0.25–1 mm fractions.

3.4. Linkages between GHG emissions and soil properties

The best subset searching revealed that NO_3^--N, DOC, BG, NAG, LAP, and po were the best explanatory variables for CO_2 and N_2O fluxes (Fig. 5), which explained approximately 54.1% of the variation in CO_2 and N_2O emissions, and 50.7% and 3.4% of information were explained with the first and second axes, respectively. The GHG emissions for the straw-amended treatments were obviously separated from those for the straw-unamended treatments. The variations in CO_2 and N_2O emissions

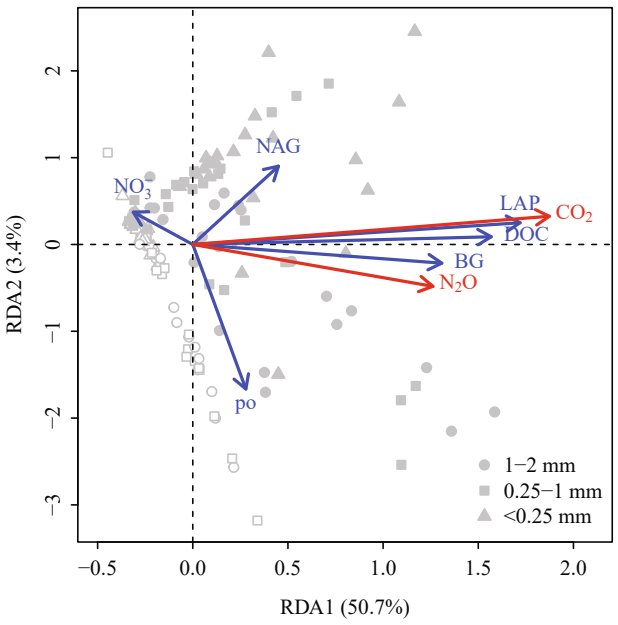

Fig. 5. Ordination plot of redundancy analysis (RDA) for the CO_2 and N_2O emissions with soil properties as constraining variables. The solid and open marks denote treatments with and without straw addition, respectively. Abbreviations: DOC, dissolved organic carbon; NO_3^--N, nitrate nitrogen; BG, β-glucosidase; LAP, leucine aminopeptidase; NAG, N-acetyl-β-D-glucosaminidase; po, phenoloxidase.

with respect to the soil DOC and NO_3^--N contents and enzyme activities were partitioned (Fig. S2). The soil DOC and NO_3^--N contributed 8.5%, whereas BG, LAP, NAG, and po contributed 18.9%. Their interactive effects had the highest contribution (24.9%) to the variation in emissions.

The PLS-SEM analysis identified the pathways mediating CO_2 and N_2O emissions (Fig. 6). The soil DOC elicited dominant direct promoting effects on CO_2 emission. The soil DOC also affected CO_2 emissions indirectly through enzyme activities. The soil NO_3^--N mainly exerted an indirect positive effect on N_2O emission through enzyme activities. The BG and po positively regulated N_2O emission but negatively controlled CO_2 emission. The N-acquiring enzymes exerted positive control on CO_2 and N_2O emissions. The three subgrouping PLS-SEMs showed that the positive impacts of N-acquiring enzyme on CO_2 emissions continued to weaken as the aggregate sizes decreased, and the promoting effects of DOC on CO_2 emissions intensified as the aggregate size decreased (Table S2).

4. Discussion

4.1. Effects of soil aggregate size and straw addition on CO_2 emissions

Consistent with previous findings (Bandyopadhyay and Lal, 2014), our results showed that CO_2 emission was strongly affected by soil aggregate sizes, and higher emissions were observed in larger aggregates in the absence of straw. This effect is probably driven by microbial activation (Zhu et al., 2014). The greater amounts of available C sources in larger aggregates (Fig. 3a) could provide more nutrients for overall microbial growth, inducing extracellular enzyme production and subsequently enhancing soil organic matter (SOM) mineralization (Zhu et al., 2014; Liao et al., 2018). Soil respiration is often linked to chemical compositions of the available C (Song et al., 2018). The organic matter in macroaggregates is less protected and more labile (Marx et al., 2005; von Lützow et al., 2006), which resulting in its easily accessed and respired by decomposer microbes. Straw addition strongly increased CO_2 emissions, and this increase was more pronounced in < 0.25 mm fraction than in 1–2 and 0.25–1 mm fractions. Consequently, the highest CO_2 emission occurred in < 0.25 mm fraction, but this finding was contrary to our hypothesis. Studies have observed that aggregate surface area increases as aggregate sizes decrease (Curtin et al., 2014). A large surface area may allow the intimate contact of straw-derived substrates and microbes (Shahbaz et al., 2017), and this observation, together with high DOC contents (Fig. 3b; Fig. 4a), could explain the higher CO_2 emission in < 0.25 mm fraction in straw-amended treatments. The highest C occurred in small aggregate (Fig. 3b; Fig. 4a) is corroborated by Zhao et al. (2018), who proposed that straw-derived C easily accumulates in small aggregate fractions. In labile C-rich surroundings, soil microbes can catabolize superfluous C via rapid microbial overflow respiration to maintain microbial stoichiometric balance (Zhu et al., 2018). Straw-derived organic particles can bond with mineral matter, and < 0.25 mm aggregate may aggregate and form a larger size after straw addition (Huang et al., 2018); thus, the diffusion limitation of the generated CO_2 in < 0.25 mm aggregate was possibly relieved. Conversely, larger aggregates can protect exogenous organic matter from mineralization because of their intense occlusion effect (Bimüller et al., 2016).

4.2. Effects of soil aggregate size and straw addition on N_2O emissions

Straw addition increased N_2O emissions in each size of aggregates, and N_2O emissions in 1–2 mm fraction ranked the first in both straw-unamended and straw-amended treatments (Fig. 2b). The increase in C and N substrates with exogenous straw addition may be attributed to the increased N_2O emissions by supplying energy to N_2O-producing microorganisms (Mehnaz et al., 2019). In the present study, the high

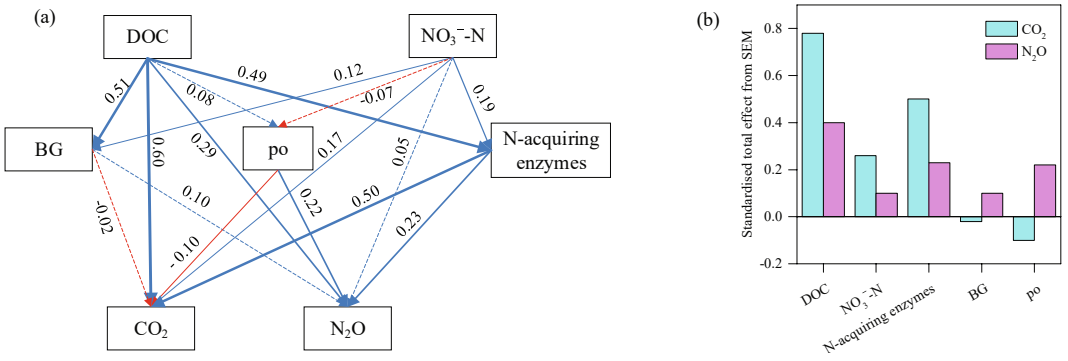

Fig. 6. The partial least squares structural equation model (PLS-SEM) for the effects of soil DOC, NO_3^--N, BG, po and N-acquiring enzyme on CO_2 and N_2O emissions. N-acquiring enzyme is a latent variable, which is indicated by LAP and NAG. Negative and positive effects are indicated by red and blue line, respectively, while non-significant effect is indicated by dashed line. The line width is proportional to the effect strength. Abbreviations: CO_2, carbon dioxide; N_2O, nitrous oxide; DOC, dissolved organic carbon; NO_3^--N, nitrate nitrogen; BG, β-glucosidase; LAP, leucine aminopeptidase; NAG, N-acetyl-β-D-glucosaminidase; po, phenoloxidase.

enzyme activities in 1–2 mm fraction (Fig. 4) could stimulate soil organic N mineralization, thereby leading to an increase in inorganic-N pool available for nitrifying and denitrifying microorganisms (White and Reddy, 2000), which were possibly responsible for the high N_2O emissions from macroaggregates. The highest NO_3^--N and the lowest NH_4^+-N indicated that nitrification might be a dominant contributor to N_2O production in 1–2 mm fraction. This finding was supported by Chen et al. (2016), who found that ammonia oxidation "hot spots" with highly localized N_2O production exist in macroaggregates because the microenvironment provides more favorable conditions, e.g., suitable oxygen (O_2), for ammonia oxidizers. Under the physical mechanism, soil porosity is a major determinant of soil aeration and transport properties, e.g., solutes, water, and gaseous substance diffusion (Mangalassery et al., 2013). Jayarathne et al. (2021) suggested that macroaggregates hold more intra- and inter-aggregate pores, for which the transport of N_2O produced in the soil to atmosphere would be more easily (Ebrahimi and Or, 2018; Mangalassery et al., 2013). Diffusion limitation in microaggregates increases the residence time of the produced N_2O in soil, it is highly likely that the generated N_2O is partially entrapped or further reduced to N_2 in < 0.25 mm fraction (Jayarathne et al., 2021; Uchida et al., 2008). In addition, the rapidly mineralized (straw plus soil) in < 0.25 mm fraction treated with straw (Fig. 1b; Fig. 2a) might have consumed large amounts of O_2, and local anoxia in microsites possibly favor the complete denitrification to N_2 because O_2 availability strongly suppresses N_2O reductase (Wrage et al., 2001).

4.3. Responses of aggregate-associated enzyme activities to straw addition

In keeping with previous works (Nie et al., 2014; Sinsabaugh et al., 2002), our results revealed that crop straw and aggregate size could strongly affect soil enzyme activities. Straw may trigger extracellular enzyme production (BG, CB, LAP, NAG, and po) in each aggregate fraction by providing a primary energy source to fuel microorganisms (Allison and Vitousek, 2005). In the presence of straw, the activities of all the tested enzymes differed among aggregate sizes. The least activities were observed in < 0.25 mm fraction during the entire incubation (Fig. S1). Enzyme activities are generally regulated by labile SOM (Allison and Vitousek, 2005). Our results also showed that enzyme activities were positively correlated with DOC concentrations; however, soil aggregate size inversely affected enzyme activities and DOC concentration. This phenomenon indicated that other factors, such as soil pore spaces and stoichiometry of soil nutrient elements (Chen et al., 2014), could also explain the lowest enzyme activities in < 0.25 mm fraction. Soil enzymes are mainly produced by soil microorganisms. The spatial distributions of microbial communities vary with aggregate size because of a complex environment within aggregates; a previous study indicated that microbial biomass and activity are lower in the interior of microaggregates (Mummey and Stahl, 2004), possibly resulting in reduced extracellular enzyme activities. The strong interaction effects of straw addition and soil aggregate size on BG, CB, and NAG (Table 2) suggested that soil extracellular enzymes within soil microhabitats were sensitive to straw addition. In addition, oxidative enzyme activities (per) were only largely determined by soil aggregate size.

4.4. Factors regulating CO_2 and N_2O emissions

CO_2 and N_2O emissions were regulated by biological (CB, LAP, NAG, and po) and abiotic (DOC and NO_3^--N) factors, and their interaction was the major determinant (Fig. S2). SEM analysis further revealed that DOC and NO_3^--N influenced CO_2 and N_2O emissions partially through a build-up of enzyme activities (Fig. 6a). Previous studies demonstrated that soil enzyme activities are sensitive indicators of microbial functions depending on nutrient availability; as soil nutrients change, microorganisms secrete extracellular enzymes to acquire nutrients from SOM (Mehnaz et al., 2019). Therefore, they can strongly affect soil C and N mineralization (Caldwell, 2005). Regarding CO_2 emissions, the soil DOC was the most important variable that had dominant effects on CO_2 emissions (Fig. 6b). The three subgrouping SEMs showed that the direct promoting effect of DOC on CO_2 was the highest in < 0.25 mm fraction (Table S2). Thus, the higher CO_2 emission from microaggregates in straw-amended treatments could be mainly explained by their higher DOC concentration. Enzyme activities played different roles in CO_2 and N_2O emissions (Fig. 6a). C-acquiring and oxidative enzyme activities contributed negatively to CO_2 emissions, and this effect was weak (Fig. 6a). As for N_2O emissions, N-acquiring, C-acquiring, and oxidative enzyme activities elicited promoting effects, suggesting that macroaggregates emitted more N_2O mainly by increasing soil enzyme activities.

4.5. Limitations and implications

This study emphasized the changes in soil CO_2 and N_2O emissions in response to

soil aggregate size with straw addition. Although emissions in different soil aggregate sizes were measured under artificial conditions, e.g., the absence of plants and fertilization or the spatial heterogeneity of the distribution of particle sizes, possibly causing different behaviors from *in situ*, it was still an improvement for understanding the spatial distribution of C mineralization and N_2O emissions. We also revealed that straw addition affected CO_2 and N_2O emissions from different soil aggregate sizes. As a result, the contribution of CO_2 and N_2O emissions from 1 to 2 and 0.25–1 mm fractions towards emissions from bulk soil decreased, but the contribution of < 0.25 mm fraction increased (Table S1). This result strengthened our understanding on the mechanisms of straw effects on GHG emissions. Considering straw returning can promote SOC sequestration in the long run (Huang et al., 2018; Liu et al., 2014), this practice possibly would offset the increase in GWP from N_2O emissions. Previous studies also confirmed that the added straw with a large C/N ratio lessens the mineralization of the added straw and SOC compared with a low C/N straw (Shahbaz et al., 2017). It can also induce microbial N assimilation and consequently limit available N substrates for N_2O-producing microorganisms (Zhou et al., 2020). In addition, aggregate dynamics are dependent on the bioavailability of straws, which have differential decomposing rates (Zhao et al., 2018). In this regard, further studies should examine aggregate-scale GHG dynamics after adding straw with different C/N ratio to a variety of soils. If possible, an isotopic labeling technique should be used to partition straw- and soil-derived CO_2 or N_2O.

5. Conclusion

This study clearly showed that CO_2 and N_2O emissions from different soil aggregate sizes were affected by straw addition. Crop straw addition accelerated CO_2 and N_2O fluxes from differently sized soil aggregates by modifying soil available C and N contents and enzyme activities. The magnitude of straw addition that increased CO_2 emission was higher in < 0.25 mm fraction than in 1–2 and 0.25–1 mm fractions. By contrast, the N_2O emission in 1–2 mm fraction in the straw-amended treatments was the highest. Most enzyme activities were enhanced by straw addition, and < 0.25 mm fraction exerted the lowest enzyme activities in the straw-amended treatments. Straw addition reduced the contribution of CO_2 and N_2O emissions from 1 to 2 and 0.25–1 mm fractions toward emissions from bulk soil but increased the contribution of < 0.25 mm fraction. These results indicated that frequent artificial disturbance in agricultural management remarkably changed the soil aggregation size distributions and might theoretically influence soil C mineralization and N_2O emissions.

Declaration of Competing Interest

The authors declare that they have no known competing financial interests or personal relationships that could have appeared to influence the work reported in this paper.

Acknowledgement

This work was supported by the National Key Research and Development program of China (No. 2017YFD0800102), and the National Natural Science Foundation of China (No. 41671253 and No. 31670506).

Appendix A. Supplementary data

Supplementary data to this article can be found online at https://doi.org/10.1016/j.geoderma.2021.115342.

References

Allison, S.D., Vitousek, P.M., 2005. Responses of extracellular enzymes to simple and complex nutrient inputs. Soil Biol. Biochem. 37, 937–944.
Bandyopadhyay, K.K., Lal, R., 2014. Effect of land use management on greenhouse gas emissions from water stable aggregates. Geoderma 232–234, 363–372.
Bimüller, C., Kreyling, O., Kölbl, A., von Lützow, M., Kögel-Knabner, I., 2016. Carbon and nitrogen mineralization in hierarchically structured aggregates of different size. Soil Till. Res. 160, 23–33.
Blake, G.R., Hartge, K.H., 1986. Bulk density. In: Klute, A. (Ed.), Methods of Soil Analysis, Part 1—Physical and Mineralogical Methods, Agronomy Monograph, 2nd Edition, 9. American Society of Agronomy—Soil Science Society of America, Madison, pp. 363–382.
Borcard, D., Legendre, P., Drapeau, P., 1992. Partialling out the spatial component of ecological variation. Ecol. Soc. 73, 1045–1055.
Bronick, C.J., Lal, R., 2005b. Soil structure and management: a review. Geoderma 124, 3–22.
Butterly, C.R., Marschner, P., McNeill, A.M., Baldock, J.A., 2010. Rewetting CO_2 pulses in Australian agricultural soils and the influence of soil properties. Biol. Fertil. Soils 46, 739–753.
Caldwell, B.A., 2005. Enzyme activities as a component of soil biodiversity: A review. Pedobiologia 49, 637–644.
Cantzler, J., Creutzig, F., Ayargarnchanakul, E., Javaid, A., Wong, L., Haas, W., 2020. Saving resources and the climate? A systematic review of the circular economy and its mitigation potential. Environ. Res. Lett. 15.
Chabbi, A., Lehmann, J., Ciais, P., Loescher, H.W., Cotrufo, M.F., Don, A., SanClements, M., Schipper, L., Six, J., Smith, P., Rumpel, C., 2017. Aligning agriculture and climate policy. Nat. Clim. Chang. 7, 307–309.
Chen, R., Senbayram, M., Blagodatsky, S., Myachina, O., Dittert, K., Lin, X., Blagodatskaya, E., Kuzyakov, Y., 2014. Soil C and N availability determine the priming effect: Microbial N mining and stoichiometric decomposition theories. Glob. Chang. Biol. 20, 2356–2367.
Curtin, D., Beare, M.H., Scott, C.L., Hernandez-Ramirez, G., Meenken, E.D., 2014. Mineralization of soil carbon and nitrogen following physical disturbance: A laboratory assessment. Soil Sci. Soc. Am. J. 78, 925–935.
Ebrahimi, A., Or, D., 2018. Dynamics of soil biogeochemical gas emissions shaped by remolded aggregate sizes and carbon configurations under hydration cycles. Glob. Chang. Biol. 24, 378–392.
Garcia-Marco, S., Ravella, S.R., Chadwick, D., Vallejo, A., Gregory, A.S., Cardenas, L.M., 2014. Ranking factors affecting emissions of GHG from incubated agricultural soils. Eur. J. Soil Sci. 65, 573–583.
Han, M., Zhu, B., 2020. Changes in soil greenhouse gas fluxes by land use change from primary forest. Glob. Chang. Biol. 26, 2656–2667.
Huang, T., Yang, H., Huang, C., Ju, X., 2018. Effects of nitrogen management and straw return on soil organic carbon sequestration and aggregate-associated carbon. Eur. J. Soil Sci. 69, 913–923.
IPCC, 2014. In: Core Writing Team, Pachauri, R.K., Meyer, L.A. (Eds.), Climate Change 2014: Synthesis Report. Contribution of Working Groups I, II and III to the Fifth Assessment Report of the Intergovernmental Panel on Climate Change (IPCC). IPCC, Geneva, Switzerland 151 pp.
IUSS Working Group WRB. 2015. World Reference Base for Soil Resources 2014, update 2015International soil classification system for naming soils and creating legends for soil maps. World Soil Resources Reports No. 106. FAO, Rome.
Jayarathne, J.R.R.N., Chamindu Deepagoda, T.K.K., Clough, T.J., Thomas, S., Elberling, B., Smits, K.M., 2021. Effect of aggregate size distribution on soil moisture, soil-gas diffusivity, and N_2O emissions from a pasture soil. Geoderma 383, 114737.
Kettler, T., Doran, J.W., Gilbert, T., 2001. Simplified method for soil particle-size determination to accompany soil-quality analyses. Soil Sci. Soc. Am. J. 65, 849–852.
Kimura, S.D., Melling, L., Goh, K.J., 2012. Influence of soil aggregate size on greenhouse gas emission and uptake rate from tropical peat soil in forest and different oil palm development years. Geoderma 185–186, 1–5.
Kool, D.M., Hoffland, E., Hummelink, E.W.J., van Groenigen, J.W., 2006. Increased hippuric acid content of urine can reduce soil N_2O fluxes. Soil Biol. Biochem. 38, 1021–1027.
Ley, M., Lehmann, M.F., Niklaus, P.A., Luster, J., 2018. Alteration of nitrous oxide emissions from floodplain soils by aggregate size, litter accumulation and plant–soil interactions. Biogeosciene 15, 7043–7057.
Li, H., Cao, Y., Wang, X., Ge, X., Li, B., Jin, C., 2017. Evaluation on the production of food crop straw in China from 2006 to 2014. BioEnerg. Res. 10, 949–957.
Li, P.-P., Han, Y.-L., He, J.-Z., Zhang, S.-Q., Zhang, L.-M., 2019. Soil aggregate size and long-term fertilization effects on the function and community of ammonia oxidizers. Geoderma 338, 107–117.
Li, P.-P., Zhang, S.-Q., Li, F., Zhang, Y.-T., Han, Y.-L., 2020. Long term combined fertilization and soil aggregate size on the denitrification and community of denitrifiers. Appl. Soil Ecol. 156, 103718.
Liao, H., Zhang, Y., Zuo, Q., Du, B., Chen, W., Wei, D., Huang, Q., 2018. Contrasting responses of bacterial and fungal communities to aggregate-size fractions and long-term fertilizations in soils of northeastern China. Sci. Total Environ. 635, 784–792.
Liu, C., Lu, M., Cui, J., Li, B., Fang, C., 2014. Effects of straw carbon input on carbon dynamics in agricultural soils: a meta-analysis. Glob. Chang. Biol. 20, 1366–1381.
Mangalassery, S., Sjögersten, S., Sparkes, D.L., Sturrock, C.J., Mooney, S.J., 2013. The effect of soil aggregate size on pore structure and its consequence on emission of greenhouse gases. Soil Till. Res. 132, 39–46.
Marx, M.C., Wood, M., Jarvis, S.C., 2001. A microplate fluorimetric assay for the study of enzyme diversity in soils. Soil Biol. Biochem. 33, 1633–1640.
Marx, M.C., Kandeler, E., Wood, M., Wermbter, N., Jarvis, S.C., 2005. Exploring the enzymatic landscape: distribution and kinetics of hydrolytic enzymes in soil particle-size fractions. Soil Biol. Biochem. 37, 35–48.
Mehnaz, K.R., Corneo, P.E., Keitel, C., Dijkstra, F.A., 2019. Carbon and phosphorus addition effects on microbial carbon use efficiency, soil organic matter priming, gross nitrogen mineralization and nitrous oxide emission from soil. Soil Biol. Biochem. 134, 175–186.
Messiga, A.J., Ziadi, N., Angers, D.A., Morel, C., Parent, L.E., 2011. Tillage practices of a clay loam soil affect soil aggregation and associated C and P concentrations. Geoderma 164, 225–231.
Mummey, D.L., Stahl, P.D., 2004. Analysis of soil whole- and inner-microaggregate bacterial communities. Microb. Ecol. 48, 41–50.
Nie, M., Pendall, E., Bell, C., Wallenstein, M.D., 2014. Soil aggregate size distribution mediates microbial climate change feedbacks. Soil Biol. Biochem. 68, 357–365.
Oksanen, J., Blanchet, F.G., Kindt, R., Legendre, P., Minchin, P.R., O'Hara, R.B., Simpson, G.L., Solymos, P., Stevens, M.H.H., Wagner, H., 2019. vegan: Community Ecology Package. R package version 2.5-6. https://CRAN.R-project.org/package=vegan.
Pilegaard, K., 2013. Processes regulating nitric oxide emissions from soils. Philos. Trans. R. Soc. B 368, 20130126. https://doi.org/10.1098/rstb.2013.0126.
R Core Team, 2020. R: A language and environment for statistical computing. R Foundation for Statistical Computing, Vienna, Austria. https://www.R-project.org/.
Reeves, S.H., Somasundaram, J., Wang, W.J., Heenan, M.A., Finn, D., Dalal, R.C., 2019. Effect of soil aggregate size and long-term contrasting tillage, stubble and nitrogen management regimes on CO_2 fluxes from a Vertisol. Geoderma 337, 1086–1096.
Robinson, A., Di, H.J., Cameron, K.C., Podolyan, A., 2014. Effect of soil aggregate size and dicyandiamide on N_2O emissions and ammonia oxidizer abundance in a grazed pasture soil. Soil Use Manag. 30, 231–240.
Sanchez, G., Trinchera, L., Russolillo, G., 2017. Plspm: Tools for Partial Least Squares Path Modeling (PLS-PM). R package version 0.4.9. https://CRAN.R-project.org/package=plspm.
Saiya-Cork, K.R., Sinsabaugh, R.L., Zak, D.R., 2002. The effects of long term nitrogen deposition on extracellular enzyme activity in an Acer saccharum forest soil. Soil Biol. Biochem. 34, 1309–1315.
Shaaban, M., Hu, R., Wu, Y., Younas, A., Xu, X., Sun, Z., Jiang, Y., Lin, S., 2019. Mitigation of N_2O emissions from urine treated acidic soils by liming. Environ. Pollut. 255, 113237.
Shahbaz, M., Kuzyakov, Y., Heitkamp, F., 2017. Decrease of soil organic matter stabilization with increasing inputs: Mechanisms and controls. Geoderma 304, 76–82.
Sinsabaugh, R.L., Carreiro, M.M., Repert, D.A., 2002. Allocation of extracellular enzymatic activity in relation to litter composition, N deposition, and mass loss. Biogeochemistry 60, 1–24.
Song, Y., Song, C., Hou, A., Ren, J., Wang, X., Cui, Q., Wang, M., 2018. Effects of temperature and root additions on soil carbon and nitrogen mineralization in a predominantly permafrost peatland. Catena 165, 381–389.
Soussana, J.-F., Lutfalla, S., Ehrhardt, F., Rosenstock, T., Lamanna, C., Havlík, P., Richards, M., Wollenberg, E., Chotte, J.-L., Torquebiau, E., Ciais, P., Smith, P., Lal, R., 2019. Matching policy and science: Rationale for the '4 per 1000 - soils for food security and climate' initiative. Soil Till. Res. 188, 3–15.
Uchida, Y., Clough, T., Kelliher, F., Sherlock, R., 2008. Effects of aggregate size, soil compaction, and bovine urine on N_2O emissions from a pasture soil. Soil Biol. Biochem. 40, 924–931.
Upton, R.N., Bach, E.M., Hofmockel, K.S., 2019. Spatio-temporal microbial community dynamics within soil aggregates. Soil Biol. Biochem. 132, 58–68.
von Lützow, M., Kögel-Knabner, I., Ekschmitt, K., Matzner, E., Guggenberger, G., Marschner, B., Flessa, H., 2006. Stabilization of organic matter in temperate soils: mechanisms and their relevance under different soil conditions—A review. Eur. J. Soil Sci. 57, 426–445.
Wang, B., Brewer, P.E., Shugart, H.H., Lerdau, M.T., Allison, S.D., 2019a. Soil aggregates as biogeochemical reactors and implications for soil-atmosphere exchange of greenhouse gases-A concept. Glob. Chang. Biol. 25, 373–385.
Wang, H., Shen, M., Hui, D., Chen, J., Sun, G., Wang, X., Lu, C., Sheng, J., Chen, L., Luo, Y.Z., Zheng, J.C., Zhang, Y., 2019b. Straw incorporation influences soil organic carbon sequestration, greenhouse gas emission, and crop yields in a Chinese rice (*Oryza sativa* L.) –wheat (*Triticum aestivum* L.) cropping system. Soil Till. Res. 195, 104377.
Wang, X., Qi, J.-Y., Zhang, X.-Z., Li, S.-S., Latif Virk, A., Zhao, X., Xiao, X.-P., Zhang, H.-L., 2019c. Effects of tillage and residue management on soil aggregates and

associated carbon storage in a double paddy cropping system. Soil Till. Res. 194, 104339.
Wang, Y., Wang, Y., 2003. Quick measurement of CH_4, CO_2 and N_2O emissions from a short-plant ecosystem. Adv. Atmos. Sci. 20, 842–844.
White, J., Reddy, K., 2000. Influence of phosphorus loading on organic nitrogen mineralization of Everglades soils. Soil Sci. Soc. Am. J. 64, 1525–1534.
Wrage, N., Velthof, G.L., van Beusichem, M.L., Oenema, O., 2001. Role of nitrifier denitrification in the production of nitrous oxide. Soil Biol. Biochem. 33, 1723–1732.
Wu, L., Zhang, W., Wei, W., He, Z., Kuzyakov, Y., Bol, R., Hu, R., 2019. Soil organic matter priming and carbon balance after straw addition is regulated by long-term fertilization. Soil Biol. Biochem. 135, 383–391.
Xi, C.F., Zhu, K.G., Zhou, M.Z., Du, G.H., Li, X.R., Zhang, S.Y., Yang, B.Q., Hou, C.Q., Tang, J.C., Zhou, C.H., 1998. Soils of China. Chinese Agriculture Press, Beijing, pp. 1–1253 (in Chinese).
Zhang, W., Zhou, H., Sheng, R., Qin, H., Hou, H., Liu, Y., Chen, A., Chen, C., Wei, W., 2021. Differences in the nitrous oxide emission and the nitrifier and denitrifier communities among varying aggregate sizes of an arable soil in China. Geoderma 389, 114970.
Zhao, H., Shar, A.G., Li, S., Chen, Y., Shi, J., Zhang, X., Tian, X., 2018. Effect of straw return mode on soil aggregation and aggregate carbon content in an annual maize-wheat double cropping system. Soil Till. Res. 175, 178–186.
Zhao, J., Chen, S., Hu, R., Li, Y., 2017. Aggregate stability and size distribution of red soils under different land uses integrally regulated by soil organic matter, and iron and aluminum oxides. Soil Till. Res. 167, 73–79.
Zhou, M., Zhu, B., Wang, X., Wang, Y., 2017. Long-term field measurements of annual methane and nitrous oxide emissions from a Chinese subtropical wheat-rice rotation system. Soil Biol. Biochem. 115, 21–34.
Zhou, W., Jones, D.L., Hu, R., Clark, I.M., Chadwick, D.R., 2020. Crop residue carbon-to-nitrogen ratio regulates denitrifier N_2O production post flooding. Biol. Fertil. Soils. 56, 825–838.
Zhu, B., Gutknecht, J.L.M., Herman, D.J., Keck, D.C., Firestone, M.K., Cheng, W., 2014. Rhizosphere priming effects on soil carbon and nitrogen mineralization. Soil Biol. Biochem. 76, 183–192.
Zhu, Z., Ge, T., Luo, Y., Liu, S., Xu, X., Tong, C., Shibistova, O., Guggenberger, G., Wu, J., 2018. Microbial stoichiometric flexibility regulates rice straw mineralization and its priming effect in paddy soil. Soil Biol. Biochem. 121, 67–76.